Obstacle Influence on High-Pressure Jets based on Computational Fluid Dynamics Simulations

Cristian Colombini[*], Valentina Busini

Politecnico di Milano - Department of Chemistry, Materials and Chemical Engineering "Giulio Natta", Via Mancinelli 7, 20131, Milano, Italy
cristian.colombini@polimi.it

In the industrial safety framework, high-pressure jets involving toxic or flammable substances represent one of the major risks. The presence of one or more obstacles affects the extent of the plume, normally to higher dimensions, which means that an open field modeling would not be conservative and that it is necessary to explicitly consider the obstacles effects. Thus, to study this kind of scenario, only a computational fluid dynamic model allows a complete and proper description of the obstacles influence on the jet behavior.

In this work, we deal with a realistic case-study of industrial interest which involves a high-pressure methane jet impinging a nearby cylindrical tank positioned in front of the jet release.

The aims of this work are to define the geometrical parameters of the scenario, to quantify their influence on the jet-obstacle interaction, with respect to the free jet case, and then to find which of them are the most relevant. Therefore, the effect of the cylindrical tank on the lower flammability limit area extent is systematically studied using computational fluid dynamics simulations, performed with ANSYS® FLUENT®.

1. Introduction

Many industrial fluids are stored and transported in gaseous form under high-pressure. For this reason, in the risk analysis framework, the modelling of high-pressure jet releases and the quantifying of their consequences play a relevant role (Busini et al., 2012). If the jet release occurs in open field, it can be considered as a free jet (Pontiggia et al., 2014) while, if an obstacle is present beside or in front of the leak, the scenario is usually known impinging jet (Schefer et al., 2009). In the latter case, if the release involves a flammable material, domino effects may be relevant (Benard et al., 2009).

From the physical point of view, the presence of an obstacle affects significantly the jet behaviour (Hall et al., 2017) in terms of turbulence, producing eddies, and affecting the jet momentum. In particular, the mixing with fresh air can be enhanced or reduced (Pontiggia et al., 2014), influencing the extent of the flammable region with respect to the one expected from the free jet (Kotchourko et al., 2014). This means that, a priori, numerical models previously developed for free jets, e.g. integral models, are not suitable for the analysis of impinging flows (Brook et al., 2003. This kind of models is able to account for physical phenomena through semi-empirical relationship depending on parameters whose values are gathered from experimental data available for open field releases (Hanna, 1994). On the other hand, distributed numerical models, such as Computational Fluid Dynamic (CFD) models, are able to account for the influence of obstacles or, more generally, of a complex geometry on the jet release (Batt et al., 2016). Therefore, to properly simulate this kind of scenario, only a CFD analysis can be feasible and reliable, at the cost of possible significant computational demand and required user knowledge (Zuliani et al., 2016). Some efforts have been spent in the past on this topic: most of the studies has investigated the influence of obstacles on high momentum jet releases (more precisely, to determine the extent of the flammable/toxic clouds (Houf and Schefer 2007)) only for specific cases (Sposato et al., 2003; Tchouvelev et al., 2007; Bénard et al., 2007; Hourri et al., 2009; Bénard et al., 2009; Hourri et al., 2011; Angers et al., 2011; Bénard et al., 2016). However, none of this literature works explicitly investigates the influence of a real 3D obstacle on the flammable area extent of a high-pressure jet with respect to the free jet case.

Therefore, in this work, the obstacle influence was investigated varying some of the geometrical key parameters of both obstacle and orifice. More specifically, a realistic case-study of industrial interest was considered. It involves a high-pressure methane jet impinging a horizontal cylindrical tank positioned in front of the jet release.

The aims of this work are:

- to define the geometrical parameters significant for this scenario;
- to quantify these parameters' influence on the jet-obstacle interaction, with respect to the free jet case;
- to define which of them are the most influential.

Therefore, the effect of the cylindrical tank on the Lower Flammability Limit (LFL) area extent is systematically studied using CFD simulations, performed with ANSYS® FLUENT® v. 18.2.

2. Materials and methods

To obtain a good quality representation of the flow field and, at the same time, a time-saving tool, all the simulations performed in this work are Reynolds Averaged Navier-Stokes (RANS) simulation. To avoid the need of resolve the boundary layer of the ground and tank surface, among the possible turbulence models available, the k-ω SST was adopted (Ansys Inc., 2017). Standard boundary conditions were used for the domain's boundaries (as summarized in Table 1 and shown in Figure 1a), except for the back, left and right side boundaries, for which particular attention was payed to model realistic wind conditions. Indeed, to consider the atmospheric conditions of an open field scenario, a velocity profile in accordance with the atmospheric class 5D was supplied to the solver through a User Defined Function (UDF) (Pontiggia et al., 2014).

3. Results and discussion

The case-study here investigated was a realistic scenario of industrial interest which involves an accidental horizontally oriented, high-pressure release of methane impinging a horizontal cylindrical tank placed in front of the leak. Guessing a spill from a huge storage tank (or a pipeline) of methane gas, the leakage can be considered as a steady state scenario. As gas conditions inside the storage, a pressure of 65 bara and a temperature of 5 °C were used, while a diameter of 1 inch was adopted as a realistic accidental hole on the facility. The methane inlet characteristics were obtained with the Birch's pseudo source model (Birch et al., 1984), whose corresponding equivalent conditions are reported in Table 2. The rest of the boundary conditions used are summarized in Table 1.

Table 1: Boundary conditions used for the case-study simulations.

Boundary	Type
Back side	Velocity inlet, v_x = 0 m/s, v_y = 0 m/s, v_z = velocity profile
Top side	Velocity inlet, v_x = 0 m/s, v_y = -1e^{-9} m/s, v_z = 5 m/s
Left side	Velocity inlet, v_x = -1e^{-9} m/s, v_y = 0 m/s, v_z = velocity profile
Ground	Adiabatic wall, 0.01 m roughness height
Central vertical plane	Symmetry (where applicable)
Right side	Velocity inlet, v_x = 1e^{-9} m/s, v_y = 0 m/s, v_z = velocity profile
Front side	Pressure outlet
Nozzle wall	Adiabatic wall, 0.001 m roughness height
Methane inlet	Mass flow inlet, 5.184 kg/s
Tank wall	Adiabatic wall, 0.001 m roughness height

Table 2: Characteristics of the methane pseudo source used in the case-study.

Characteristic	Value
Expanded diameter	0.1458 m
Velocity	440.6 m/s
Mass flow rate	5.184 kg/s
Total Temperature	70.3 °C
Pressure	101,325 Pa

As done by Pontiggia and coworkers (Pontiggia et al., 2014), to take into account the surrounding of the release, i.e. the open field atmospheric conditions, a neutral stability class, namely atmospheric class D, with 5

m/s wind at 10 m from the ground was considered. The dimensions of the simulated domain were 70·10·10 (in m) while the obstacle was modelled as a horizontal cylinder of 5 m length and 1.7 m diameter. Notice that the domain dimensions were chosen such that the prescription for the domain extension for CFD analysis of urban environment were fulfilled (Franke et al., 2007). Figure 1a shows a representation of the simulated domain, highlighting the boundary conditions.

The free jet scenario, for which neither the ground nor the obstacle influence occurs, was performed with the aim of obtaining a reference result for comparison purposes. To be in the aforementioned situation, the nozzle was positioned at a height of 5 m and the obstacle wasn't placed (in this case, the maximum LFL extension reached is 15.54 and 1 m in z and x, respectively). The performing of the free jet scenario evidently seems of great importance to understand when and how the jet is influenced. Notice that, a grid independence analysis of the results was conducted at this stage. The initial mesh adopted ($6.08 \cdot 10^6$ cells) was tested with other two meshes, one of about $5 \cdot 10^6$ cells and the other of about $7 \cdot 10^6$ cells; all the three results were comparable. As geometric key parameters (see Figure 1b), the distance of the obstacle from the jet orifice (D), the height of the orifice above ground (H), the rotation (α) and the displacement (S) of the tank with respect to the jet axis were chosen. Therefore, an array of simulation was conducted varying one (or in some cases two) per time the geometric parameters.
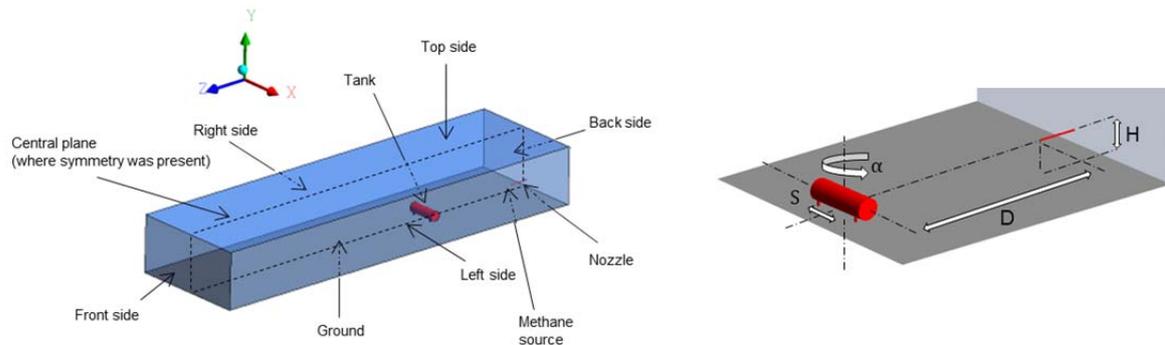

Figure 1: a) Computational domain represented as a full 3D; b) Geometric key parameters

Table 3 reports the details of all the simulation performed. As reported, each of the geometric parameters was varied of a certain amount with respect to a reference simulation which is, in most of the cases, simulation 0 (sim0). By way of example, let consider simulation 1 (sim1 in the table): the varied parameter is D, which is enhanced of the 75 % with respect to sim0. Practically, the reference simulation corresponds to the guess value of the geometric parameters, where D = 17.9 m, H = 1 m, α = 0 °, S = 0 m. The initial value of D and H were derived from the results of another preliminary simulation, in which the obstacle is not present but there is the influence of the ground (H = 1 m): 17.9 m is the half of the LFL extent (in the z axes) obtained in this case. The guess value of the other parameters, namely α and S, was arbitrarily chosen.

Table 3: Details of all the simulations performed.

	Ref.	Parameter	Variation		Ref.	Parameter	Variation
sim1	sim0	D	+75 %	sim13	sim0	α	+75 %
sim2	sim0	D	+50 %	sim14	sim0	α	+50 %
sim3	sim0	D	+25 %	sim15	sim0	α	+25 %
sim4	sim0	D	-25 %	sim16	sim0	S	+75 %
sim5	sim0	D	-50 %	sim17	sim0	S	+50%
sim6	sim0	D	-75 %	sim18	sim0	S	+25 %
sim7	sim0	H	+75 %	sim19	sim0	D	+500 %
sim8	sim0	H	+50 %	sim20	sim19	H	+75 %
sim9	sim0	H	+25 %	sim21	sim19	H	-75 %
sim10	sim0	H	-25 %	sim22	free jet	D	-50 %
sim11	sim0	H	-50 %	sim23	sim22	D	+75 %
sim12	sim0	H	-75 %	sim24	sim22	D	-75 %

Notice that, in sim13 to 18 there is no symmetry of the geometry and, therefore, the computational domain has to be a full 3D one, as shown in Figure 1a. In all other simulations, only half domain, with a symmetry condition, was considered. In Table 3 there are missing simulations: these are not reported given that their

results can be deduced by those of sim13 to 18 just mirroring them with respect to the jet axis. As aforementioned, some simulations (sim19 to sim24) were performed combining two parameter variations per time. These were selected to point out cases in which the obstacle or the ground influence were individually shown. In sim19 the obstacle is placed far enough such that the only ground influence is achieved, and the height of the jet corresponds to the one of sim0. sim20 and 21 were set, with respect to sim19, varying the jet height as reported in Table 3. While, to account only for the obstacle influence, sim22 corresponds to the situation in which the obstacle is placed in the middle of the LFL maximum extent in z of the free jet case and the height of the obstacle is 5 m, equal to the one of the orifice. As reported in Table 3, sim23 and 24 were then referred to sim22 instead of sim0. A way to show most information of the simulation results is to graph them into a 3D plot (Figure 2), where a dimensionless area A is plotted over two dimensionless spatial coordinates: in detail, the dimensionless A is defined as the ratio $A_{sim\#}/A_{free\ jet}$, where $A_{sim\#}$ is the product of the LFL maximum extent in x ($X_{sim\#}$) times the LFL maximum extent in z ($Z_{sim\#}$), and the same goes for $A_{free\ jet}$ in the free jet case. However, to ease the results interpretation, two projections are reported in Figure 3a (side view) and 3b (top view). The dimensionless X is the ratio $X_{sim\#}/X_{free\ jet}$ and Z is $Z_{sim\#}/Z_{free\ jet}$, where $X_{free\ jet}$ is the LFL maximum extent in x and $Z_{free\ jet}$ in z for the free jet case.
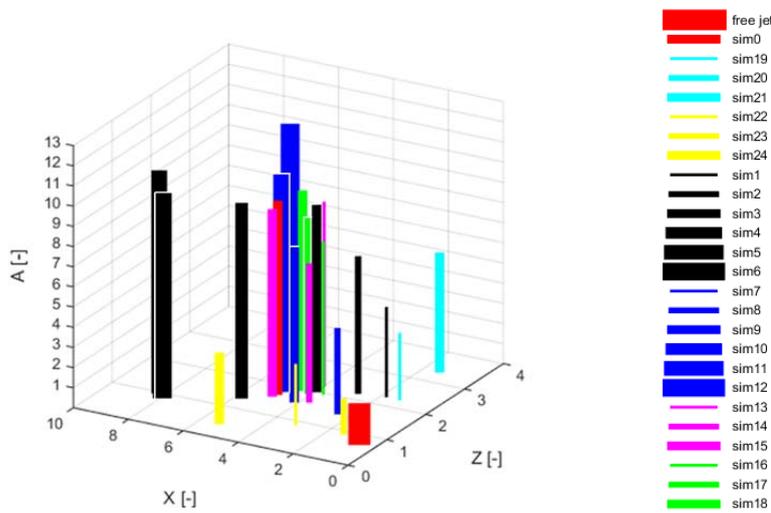

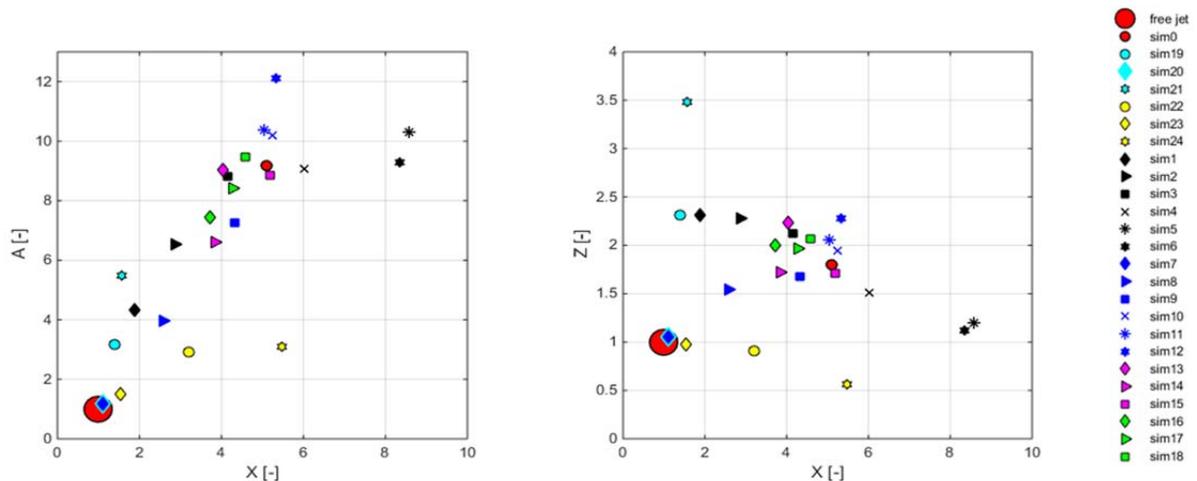
Figure 2: 3D plot of the simulations results

Figure 3: a) Side view of the 3D plot; b) Top view of the 3D plot

From Figure 3b it is possible to state that, except for sim7 and sim20, for all the other simulations an influence of the obstacle and/or the ground is noticeable. This is correct since, in sim7 and 20, the distance of the

obstacle and the height of the orifice are such that practically no influence occurs. Paying attention to the maximum extents, from Figure 3b it is appreciable that the maximum axial extent is 3.5 times the free jet one (sim21), while the transverse maximum extent is about 8.5 times the free jet case (sim5). Furthermore, it becomes clear that more the jet is crosswise extended, less it is axially, and vice versa. In terms of area A, it appears to be larger when the jet is extended in X rather than when extended in Z. In particular, the largest influence with respect to the free jet is obtained for sim12 (see Figure 2 and 3a). Both from Figure 2 and 3b, it is possible to see that about the 60 % of the results are grouped into a small region of the plane X, Z, ranging from 2 to 6 and from 1.5 to 2.5 in X and Z, respectively. Lastly, sim1 to sim6 and sim7 to sim12 seems to be aligned each other (see Figure 3b). Moreover, in terms of A, such an alignment follows an ascending order (see Figure 2 and Figure 3a).

4. Conclusions

A high-pressure release of a flammable material is considered in the present work. In this case, it is known that domino effects can occur, and that they can be relevant from the safety point of view. If an obstacle is present in the area covered by the jet, it has been stated that an influence on the release behaviour appears. In particular, the main effect seems to be the enhancement, or the reduction, of the mixing with fresh air. To account for such an influence, all the geometric features present in the domain have to be taken into account and properly modelled.

In order to investigate this kind of scenario, in this paper a CFD solver was used to model a realistic high-pressure methane release impinging on a 3D realistic obstacle placed in front of the leak.

The aims of the study were fulfilled:

- the geometric key parameters of the scenario were defined: the distance of the obstacle from the jet orifice (D), the height of the orifice above ground (H), the rotation (α) and the displacement (S) of the tank with respect to the jet axis were chosen as geometric key parameters;
- with respect to the free jet case, the quantification of all the chosen geometric parameters influence was achieved in terms of Z, X and A. As shown in Figure 3a and 3b the ground evidently affects more the axial extent rather than the transverse one. On the other way around, the prevalent obstacle effect is the enhancement of the crosswise extension with respect to the free jet. When both the obstacle and the ground influence is present, it is noticeable that, in terms of X and Z (see Figure 3b), the obstacle effect is about twice the ground one. Indeed, most of the results are grouped into a small region of the plane X, Z (around the point of coordinates X = 4.5 and Z = 2). Although their opposite effect, as the obstacle and the ground influence become stronger, A increases too. Another interesting aspect deducible from the results is that an alignment of the results, in which D and H are respectively varied, can be seen. In particular, seems that: i) there is a proportional link between D and Z, ii) there is an inverse proportional link between D and X, iii) there is an inverse proportional link between H and both Z and X.
- state that one specific geometric parameter is the most relevant could be misleading. Indeed, as aforementioned, depending on which coordinate (Z, X or A) one considers, the maximum absolute influence on the free jet can be linked to a different geometric parameter: i) considering the absolute maximum Z, H is the most relevant parameter if only the ground effect is taken into account, while H, D and α have the same effect if both ground and obstacle effects are present, ii) considering the maximum influence in terms of X, D is the most relevant parameter, iii) considering the maximum influence in terms of A, H is the most relevant parameter.

Finally, given the source conditions, the specifics of the obstacle dimensions and position and the analytical models available for the free jet case, this work can be seen as the starting point for the development of a criterion that allows the user to estimate the expected damage area (and its distribution) for the jet-obstacle interaction case.

References

Angers B., Hourri A., Bénard, P., Tchouvelev A., 2011, Numerical Investigation of a Vertical Surface on the Flammable Extent of Hydrogen and Methane Vertical Jets, International Journal of Hydrogen Energy, 36(3), 2567-72.

Ansys®, Release 18.2, Fluent User's Guide, 2017, ANSYS, Inc.

Baklanov A., Barmpas P., Bartzis J., Batchvarova E., Baumann-Stanzer K., Berkowicz U., Borrego C., Britter A., Brzozowski K., Burzynski J., Costa A.M, Carissimo C., Dimitrova R., Franke J., Grawe D., Goricsan I., Hellsten A., Janour Z., Karppinen A., Ketzel M., Krajcovicova J., Leitl B., Martilli A., Moussiopoulos N., Neophytou M., Olesen H., Papachristodoulou C. Papadakis M., Piringer M., Di Sabatino S., Sandberg M.,

Schatzmann M., Schlünzen H., Trini-Castelli S., 2007, Cost Action 732 Quality Assurance and Improvement of Microscale Meteorological Models, Brussels, Belgium.

Batt R., Gant S., Lacome J., Truchot B., 2016, Modelling of Stably-Stratified Atmospheric Boundary Layers with Commercial CFD Software for use in Risk Assessment, Chemical Engineering Transactions, 48, 61-66 DOI:10.3303/CET1648011

Bénard P., Tchouvelev A.V., Hourri A., Chen Z., Angers B., 2007, High Pressure Hydrogen Jets in the Presence of a Surface, Proceedings of the International Conference on Hydrogen Safety, 11–13 September, San Sebastain, Spain.

Bénard P., Hourri A., Angers B., Tchouvelev A., Agranat V., 2009, Effects of Surfaces on the Flammable Extent of Hydrogen Jets, Proceedings of the 3rd International Conference on Hydrogen Safety, 16-18 September, Ajaccio, Corsica.

Bénard P., Hourri A., Angers B., Tchouvelev A., 2016, Adjacent Surface Effect on the Flammable Cloud of Hydrogen and Methane Jets: Numerical Investigation and Engineering Correlations, International Journal of Hydrogen Energy, 41, 18654-662.

Birch A.D., Brown D.R., Dodson M.G., Swaffield F., 1984, The Structure and Concentration Decay of High-Pressure Jets of Natural Gas, Combustion Science and Technology, 36, 249-261.

Brook D. R., Felton N. V., Clem C. M., Strickland D. C. H., Griffiths I. H., Kingdon R. D., 2003, Validation of the Urban Dispersion Model (UDM), International Journal of Environment and Pollution, 20, 11-21.

Busini V., Massimiliano L., Rota R., 2012, Influence of Large Obstacles and Mitigation Barriers on Heavy Gas Cloud Dispersion: A Liquefied Natural Gas Case-Study, Industrial and Engineering Chemistry Research, 51, 7643–50.

Hall J.E., Hooker P., O'Sullivan L., Angers B., Hourri A., Bernard P., 2017, Flammability Profiles Associated with High-Pressure Hydrogen Jets Released in Close Proximity to Surfaces, international journal of hydrogen energy, 42, 7413-21.

Hanna S. R., 1994, Hazardous Gas-Model Evaluations - Is an Equitable Comparison Possible, Journal of Loss Prevention in the Process Industries, 7, 133-138.

Houf W., Scheffer R., 2007, Predicting Radiative Heat Flux and Flammability Envelopes from Unintended Releases of Hydrogen, International Journal of Hydrogen Energy, 32, 136-151.

Hourri A., Angers B., Bénard P., 2009, Surface Effects on Flammable Extent of Hydrogen and Methane Jets, International Journal of Hydrogen Energy, 34, 1569-1577.

Hourri A., Angers B., Bénard P., Tchouvelev A., Agranat V., 2011, Numerical Investigation of the Flammable Extent of Semi-Confined Hydrogen and Methane Jets, International Journal of Hydrogen Energy, 36, 2567-2572.

Kotchourko A., Baraldi D., Bénard P., Eisenreich N., Jordan T., Keller J., ... & Tchouvelev A., 2014, State of the Art and Research Priorities in Hydrogen Safety, Joint Research Centre of the European Commission (JRC), Honolulu, Hawaii, 2014.

Pontiggia M., Busini V., Ronzoni M., Uguccioni G., Rota R., 2014, Effect of Large Obstacles on High Momentum Jets Dispersion, Chemical Engineering Transactions, 36, 523-528 DOI: 10.3303/CET1436088.

Schefer R., Groethe M., Houf W.G., Evans G., 2009, Experimental Evaluation of Barrier Walls for Risk Reduction of Unintended Hydrogen Releases, International Journal of Hydrogen Energy, 34, 1590-1606.

Sposato C., Tamanini F., Rogers W.J., Mannan M.S., 2003, Effect of Plate Impingement on the Flammable Volume of Fuel Jet Releases, Process Safety Progress 22, 201, 2003.

Tchouvelev A. V., Cheng Z., Agranat V. M., Zhubrin S. V., 2007, Effectiveness of Small Barriers as Means to Reduce Clearance Distances, International Journal of Hydrogen Energy, 32, 1409-1415.

Zuliani C., De Lorenzi C., Ditali S., 2016, Application of CFD Simulation to Safety Problems – Challenges and Experience Including a Comparative Analysis of Hot Plume Dispersion from a Ground Flare, Chemical Engineering Transactions, 53, 79-84 DOI: 10.3303/CET1653014.